ACS APPLIED MATERIALS & INTERFACES

Research Article

www.acsami.org

Adsorption of Polycyclic Aromatic Hydrocarbons (Fluoranthene and Anthracenemethanol) by Functional Graphene Oxide and Removal by pH and Temperature-Sensitive Coagulation

Caili Zhang,[†,‡] Lin Wu,[†,‡] Dongqing Cai,[‡] Caiyun Zhang,[§] Ning Wang,[‡] Jing Zhang,[‡] and Zhengyan Wu[‡,*]

[‡]Key Laboratory of Ion Beam Bioengineering, Hefei Institutes of Physical Science, Chinese Academy of Sciences, Hefei 230031, People's Republic of China

[§]Anhui University of Traditional Chinese Medicine, Hefei 230038, People's Republic of China

Supporting Information

ABSTRACT: A new kind of functional graphene oxide with fine stability in water was fabricated by mixing graphene oxide (GO) and brilliant blue (BB) with a certain weight ratio. The adsorption performance of this mixture of BB and GO (BBGO) to polycyclic aromatic hydrocarbons (anthracenemethanol (AC) and fluoranthene (FL)) was investigated, and the results indicated BBGO possessed adsorption capacity of 1.676 mmol/g and removal efficiency of 72.7% as to AC and adsorption capacity of 2.212 mmol/g and removal efficiency of 93.2% as to FL. After adsorption, pH and temperature-sensitive coagulation (PTC) method was used to remove the AC/BBGO or FL/BBGO complex and proved to be an effective approach to flocculate the AC/BBGO or FL/BBGO complex into large flocs, which tended to be removed from the aqueous solution.

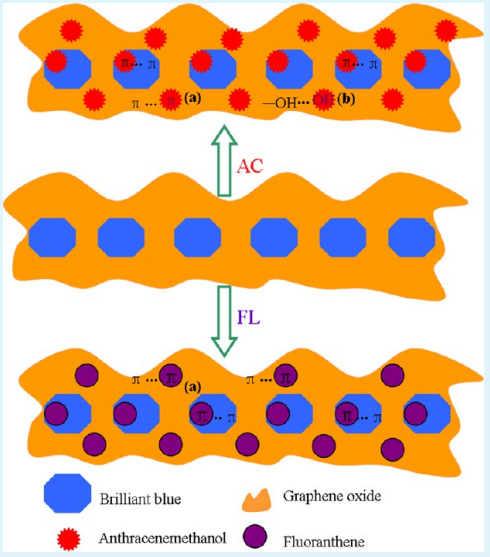

KEYWORDS: *graphene oxide, brilliant blue, anthracenemethanol, fluoranthene, adsorption, coagulation*

1. INTRODUCTION

Polycyclic aromatic hydrocarbons (PAHs) are a kind of aromatic hydrocarbons with two or more fused benzene rings from natural as well as anthropogenic sources. They are widely found in air, water, and soil, and can remain in the environment for months or years. Possible long-term health effects caused by exposure to PAHs include cataracts, kidney and liver damage and jaundice. There are several hundred different PAHs combinations, wherein up to 28 compounds have been identified as hazardous contaminants in January 2008 by the U.S. Environmental Protection Agency. For a long time, PAHs treatment has been one of the hottest issues in scientific research.[1−7]

Recently, some materials as mesoporous organosilica,[8] lightweight expanded clay aggregate,[9] petroleum coke-derived porous carbon,[10] inorgano-organo-bentonite,[11] actived carbon,[12] and nanocomposite,[13] especially carbon nanocomposite[14] as graphene oxide (GO),[15] and some new methods such as heterogeneous catalyzed oxidation,[16] enzyme degradation (immobilized by electrospun fibrous membranes),[17] activated sludge treatment,[18] combined surfactant-aided soil washing process, and coagulation treatment[19] have been used in the removal of PAHs. Among those, GO attracted extensive attention in the control of PAHs because of its high specific surface area (SSA) and solubility in aqueous solution. Additionally, GO can react with PAHs through $\pi-\pi$ interactions.[20−22] Nevertheless, the insufficient dispersion of GO in aqueous solution has been the major limit for its adsorption performance. Therefore, how to improve the dispersion of GO was significant to increase its adsorption capacity. Furthermore, after adsorption, solid-liquid separation was always achieved through filtration, precipitation, centrifugation and flocculation and so on. Therein, flocculation was generally used because of the high removal efficiency. However, it was necessary to add flocculant to the system, which might cause secondary pollution. Therefore, it was important to

Received: January 21, 2013
Accepted: April 30, 2013
Published: April 30, 2013

   dx.doi.org/10.1021/am4002666 | ACS Appl. Mater. Interfaces 2013, 5, 4783−4790

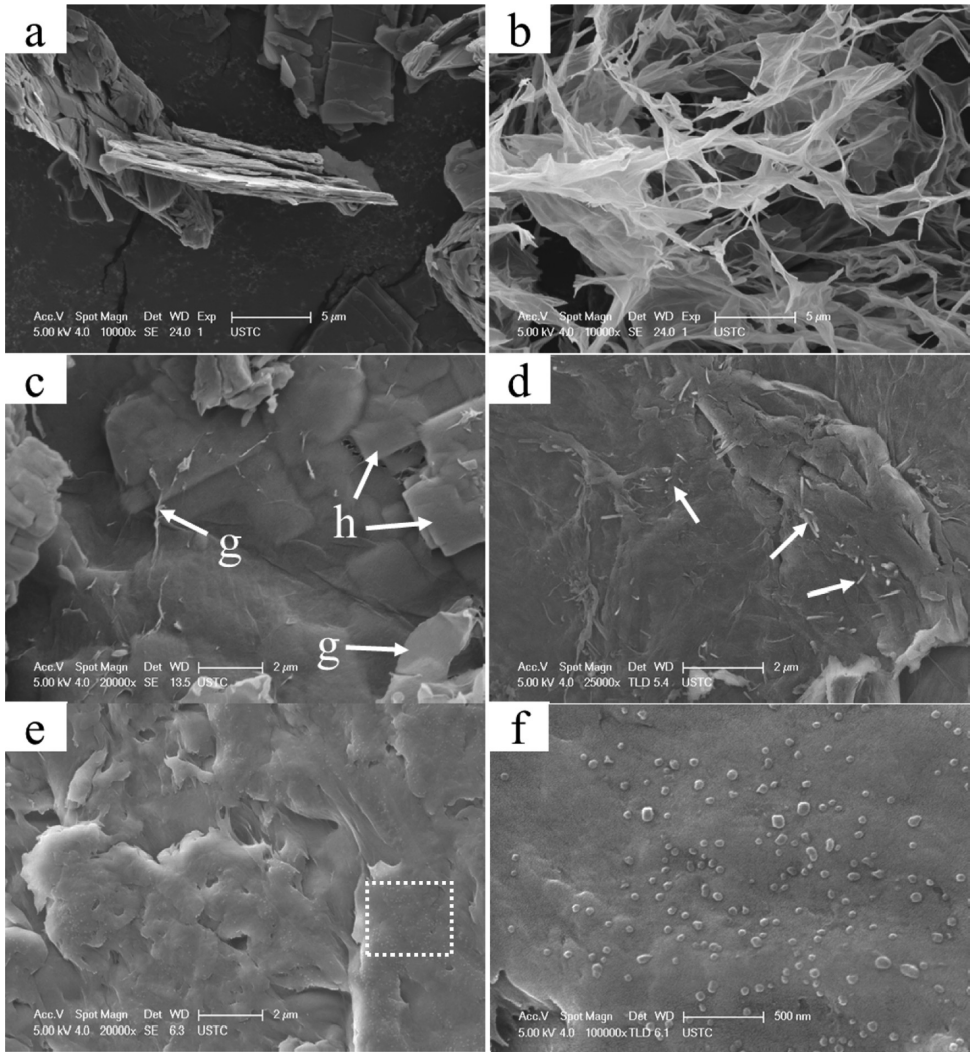

Figure 1. SEM images of (a) graphite, (b) GO, (c) BBGO, (d) AC/BBGO, (e) FL/BBGO, and (f) magnification of the marked rectangle region in e.

develop a new flocculation method without introduction of any flocculant.

In this paper, a new kind of functional graphene oxide was fabricated by mixing GO with brilliant blue (BB) in a certain proportion. It indicated that the resulting mixture of BB and GO (BBGO) showed an outstanding dispersion and stability in aqueous solution. Then the adsorption characteristics of BBGO on PAHs were investigated. As two kinds of typical PAHs, anthracenemethanol (AC) and fluoranthene (FL) were chosen as the pollutants in adsorption process. The results demonstrated that BBGO owned high adsorption capacities for both AC and FL. In addition, a facile solid-liquid separation approach was developed to remove the AC/BBGO or FL/BBGO complex, which could be adjusted by pH and temperature of the solution. The results illustrated that after adsorption, the AC/BBGO or FL/BBGO complex could be flocculated into large flocs at proper pH and temperature, which tended to be removed thereafter. It needed no addition of any flocculant to the solution, and thus could cause no secondary pollution.

2. EXPERIMENTAL SECTION

2.1. Materials. Anthracenemethanol was purchased from Adamas Reagent Co., Ltd. (Shanghai, China). Fluoranthene, graphite, brilliant blue and all the other reagents were supplied by Sinopharm Chemical Reagent Co., Ltd. (Shanghai, China). All the reagents were of analytical grade and used without further purification.

2.2. Synthesis of BBGO. Graphene oxide (GO) was prepared by modified Hummers' method.[23] Afterward, GO suspension (1 mg/mL) was prepared through 1 h ultrasonic treatment, and then a certain volume of BB solution (1 mg/mL) was added to the GO suspension. After sonicating for 40 min, BBGO complex, a new kind of functional graphene oxide, was obtained.[20]

2.3. Measurements. Zeta potential measurements were performed using a zetasizer (Zetasizer 3000, Malvern Instruments, UK). Atomic force microscopic (AFM) images were carried out using a Nanoscope III amultimode atomic force microscope (Veeco Instruments, USA). The surface morphology of sample was observed by field emission scanning electron microscope (Sirion200, FEI Co., USA). The BET specific surface area of GO or BBGO was measured using a thermal analysis instrument (Micromeritics Co., USA). The interaction analysis was performed using a Fourier transform infrared spectrometer (Bruker Co., Germany) and a Raman measurement system (Jobin Yvon Co., France). The concentration of AC or FL in aqueous solution was recorded using a UV−vis spectrophotometer (UV 2550, Shimadzu Co., Japan) at wavelength of 253 or 235 nm.

dx.doi.org/10.1021/am4002666 | ACS Appl. Mater. Interfaces 2013, 5, 4783−4790

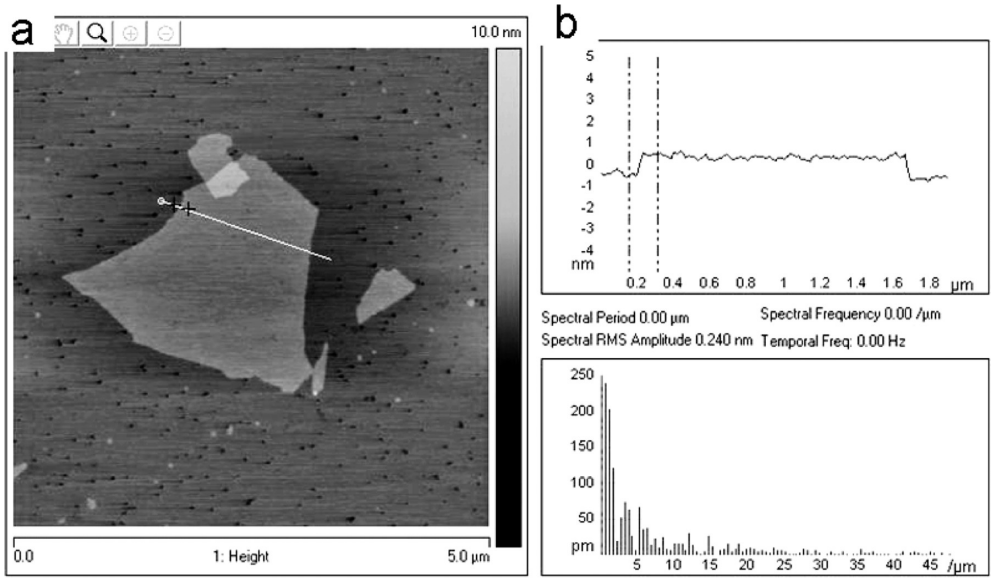

Figure 2. (a) AFM image of GO, (b) the thickness analysis.

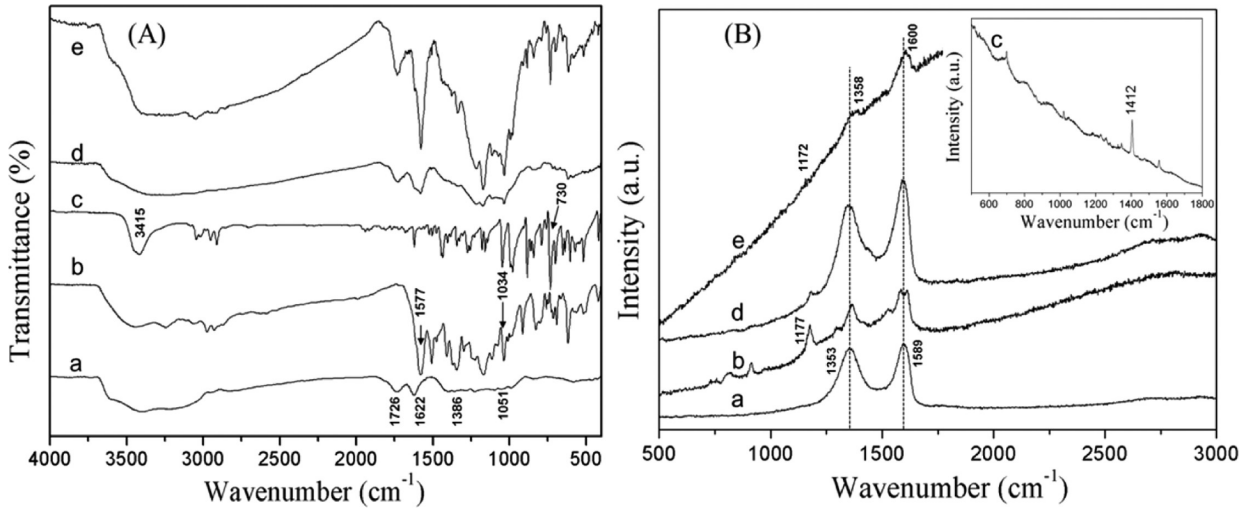

Figure 3. (A) FTIR spectra of (a) GO, (b) BB, (c) AC, (d) BBGO, and (e) AC/BBGO. (B) Raman spectra of (a) GO, (b) BB, (c) AC, (d) BBGO, and (e) AC/BBGO.

2.4. Adsorption of Anthracenemethanol or Fluoranthene onto BBGO. Adsorption experiments were carried out in batch mode at 25 °C and pH 7.0. The adsorption ability of three adsorbents (BB (1 mg/L), GO (24 mg/L) and BBGO (25 mg/L)) was studied with initial AC concentration of 10 mg/L and initial FL concentration of 10 mg/L. Samples containing AC were shaken for 11 days at the stirring speed of 150 rpm. Samples containing FL were shaken for 100 min at the stirring speed of 150 rpm.

2.5. Removal of AC/BBGO or FL/BBGO Complex after Adsorption. After adsorption, the system was heated at 60 °C and pH 3.0 for 10 min to make AC/BBGO or FL/BBGO flocculated into large flocs. After that, AC/BBGO or FL/BBGO flocs were removed through coagulation. Moreover, concentration of AC or FL remained in the supernatant was analyzed.

3. RESULTS AND DISCUSSION

3.1. Morphology Investigation and Interaction Analysis. The morphologies of graphite, GO, BBGO, AC/BBGO and FL/BBGO were observed and compared. From the SEM images in Figure 1, it could be seen that the morphology of GO was obviously different from that of graphite. GO showed a sheet-like appearance (Figure 1b) rather than the block-shaped morphology of graphite (Figure 1a). In addition, the AFM image illustrated that the GO sheet was one layer with the thickness of approximately 1 nm (Figure 2b), resulting in its high transparency and flexibility as well as SSA. This GO morphology matches well with those reported previously,[24,25] indicating that GO was successfully fabricated from graphite. In addition, BBGO showed a different appearance (Figure 1c) compared with GO, for GO sheets (noted by the arrow g in Figure 1c) becoming smooth and having BB aggregations (noted by the arrow h in Figure 1c) attached on them probably through $\pi-\pi$ interaction. During the adsorption process, AC molecules could form a number of rod-like assemblies (noted by the arrows in Figure 1d) which were thereafter adsorbed on the surface of BBGO. While FL molecules formed well-distributed small spherical particles with diameter of 50 nm approximately (indicated by the arrows in Figure 1e, f) onto the surface of BBGO.

To obtain the interaction among the components of the system (GO, BB, and AC), the FTIR analysis was carried out.

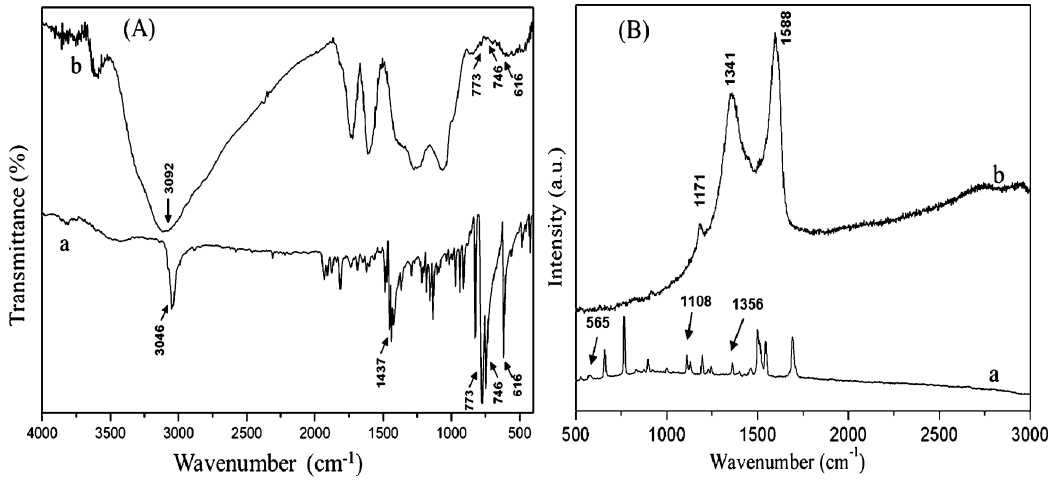

Figure 4. (A) FTIR spectra of (a) FL and (b) FL/BBGO. (B) Raman spectra of (a) FL and (b) FL/BBGO.

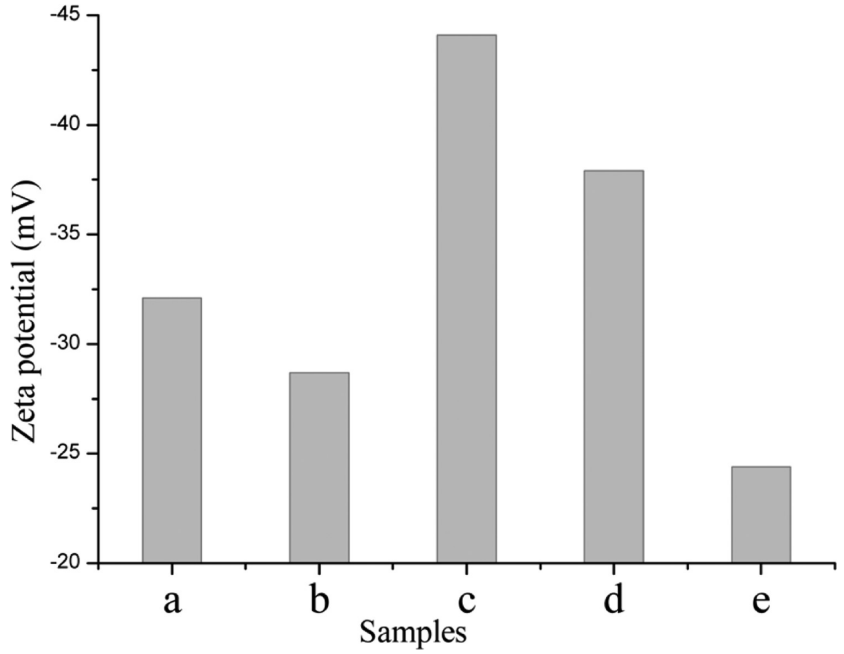

Figure 5. Zeta potentials of various systems at 30 °C. (a) GO (1 mg/L) at pH 7.0; (b) GO (1 mg/L) at pH 3.0; (c) BB (0.0417 mg/L) at pH 7.0; (d) BBGO (1.0417 mg/L) at pH 7.0; (e) BBGO (1.0417 mg/L) at pH 3.0.

As to GO, the peaks at 1726, 1622, 1386, and 1051 cm^{-1} corresponded to the vibrations of C═O, C−OH, C═C and C−O−C, respectively (Figure 3A, line a), which could be also seen in the spectrum of BBGO, except the peak of 1622 cm^{-1} showed a weak shift to 1616 cm^{-1} (Figure 3A, line d). Additionally, the peaks at 1577 cm^{-1} (C═N vibration) and 1034 cm^{-1} (−OH vibration) of BB (Figure 3A, line b) also existed in the spectra of BBGO and AC/BBGO. These results demonstrated that BBGO was successfully obtained through the interaction force between GO and BB. Furthermore, in the spectrum of AC/BBGO, the characteristic peaks of AC (Figure 3A, line c) at 3415 and 730 cm^{-1} (−OH vibrations) could be also found, indicating that AC was adsorbed on BBGO. Meanwhile, the narrow peak at 3415 cm^{-1} of AC changed into broad peak in the spectrum of AC/BBGO, and the peak at 1625 cm^{-1} of AC shifted to 1583 cm^{-1} in the spectrum of AC/BBGO, indicating the formation of hydrogen bond.[26,27] The interaction between BBGO and FL was investigated by FTIR as well. The peaks at 773 and 746 cm^{-1} corresponded to the out of plane vibration of C−H of FL (Figure 4A, line a), which could be also found in the spectrum of FL/BBGO (Figure 4A, line b), indicating that FL was successfully adsorbed onto the BBGO.

The Raman spectra of GO, BB, AC, BBGO, and AC/BBGO were displayed in Figure 3B. GO showed two peaks at 1589 and 1353 cm^{-1} corresponding to the G and D bands, respectively. Compared with the spectrum of BB, the feature at 1177 cm^{-1} appearing in the spectrum of BBGO could be assigned to BB absorbed onto GO. As to AC, the feature at 1412 cm^{-1} disappeared in the spectrum of AC/BBGO, probably for the occurring of $\pi-\pi$ interaction between AC and BBGO, which could significantly influence the Raman vibration of AC.[28] From the Raman spectra of FL and FL/BBGO (shown in Figure 4B), it could be seen that all features at 1356, 1108, and 565 cm^{-1} of FL disappeared in the spectrum of FL/BBGO, possibly for the formation of new $\pi-\pi$

interaction between FL and BBGO, which could significantly influence the Raman vibration of FL.

The SSA of GO or BBGO was measured and the results illustrated that BBGO owned higher SSA compared with GO (see Figure S1 in the Supporting Information). Besides the SSA, the stability of BBGO in the aqueous solution was another significant factor affecting the adsorption capacity. Hence, the improvement of the BBGO stability was essential to increase its adsorption performance. The stability of GO or BBGO in aqueous solution was investigated for 11 days, and the results demonstrated that BBGO in aqueous solution was more stable than GO (see Figure S2 in the Supporting Information). Besides, according to DLVO theory,[29] the zeta potential (ZP) of the BBGO colloids was closely related to the stability due to the electrostatic repulsion among the BBGO colloidal particles. Higher zeta potential (absolute value) implied farther mean distance among the particles and thus better stability (ASTM D4187−82). As seen from Figure 5, because of the high ZP of BB, the ZP of BBGO containing BB was higher than that of GO at pH 7.0, which implied that BBGO was more stable in aqueous solution compared with GO. This result demonstrated that BB could significantly increase the stability of GO at pH 7.0, which was beneficial to improve the adsorption ability of GO. Nevertheless, at pH 3.0, the result was reverse, presenting that the stability of BBGO was lower than that of GO. That was to say, compared with GO, BBGO tended to be destabilized at pH 3.0 and form flocs which could precipitate easily thereafter. Hence, the coagulation of BBGO could be controlled conveniently by pH of the solution without addition of any flocculant, so that no secondary pollution was introduced to the system.

3.2. Optimization of Experimental Variables. The influences of three factors (weight ratio of BB to GO (W_{BB}:W_{GO}), pH and temperature) on the coagulation of BBGO were investigated. As to the weight ratio optimization, coagulation phenomenon appeared at all tested ratios of W_{BB}:W_{GO} (24:1, 8:1, 4:1, 1:1, 1:4, 1:8, and 1:24) under experimental conditions. However, as shown in Figure 6a, different amounts of BB and GO still existed in the supernatant after coagulation at weight ratios of 24:1, 8:1, 4:1, and 1:1, in the meantime there was no BB or GO remaining in the aqueous solution at ratio of 1:4, 1:8 and 1:24, which means no second pollution was introduced at these three ratios. Among these three ratios, the addition amount of BB in W_{BB}:W_{GO} of 1:24 was the smallest. Consequently, 1:24 was chosen as the optimal weight ratio of BB to GO for the coagulation of BBGO.

Coagulation of BBGO in the solution was significantly influenced by pH, and the coagulation just occurred at pH lower than 5.0. This was because higher pH caused higher ZP absolute value of BBGO colloidal particles and thus lower coagulation efficiency. With the increase of pH from 1.0 to 7.0, after coagulation, BB residue ratio in the supernatant increased significantly from 0 to about 100% and kept around 100% thereafter. From Figure 6b, little GO remained in the supernatant from pH 1.0 to 3.0, whereas the GO residue increased substantially thereafter. Therefore, only at pH 1.0 and 3.0, neither BB nor GO remained in the supernatant after coagulation. Considering the strong acidity at pH 1.0, pH 3.0 might be better, so pH 3.0 was selected as optimum condition for the coagulation of BBGO.

Additionally, the influence of temperature on the coagulation of BBGO was also investigated. From Figure 6c, it was obvious that both BB and GO residue decreased with the increase of

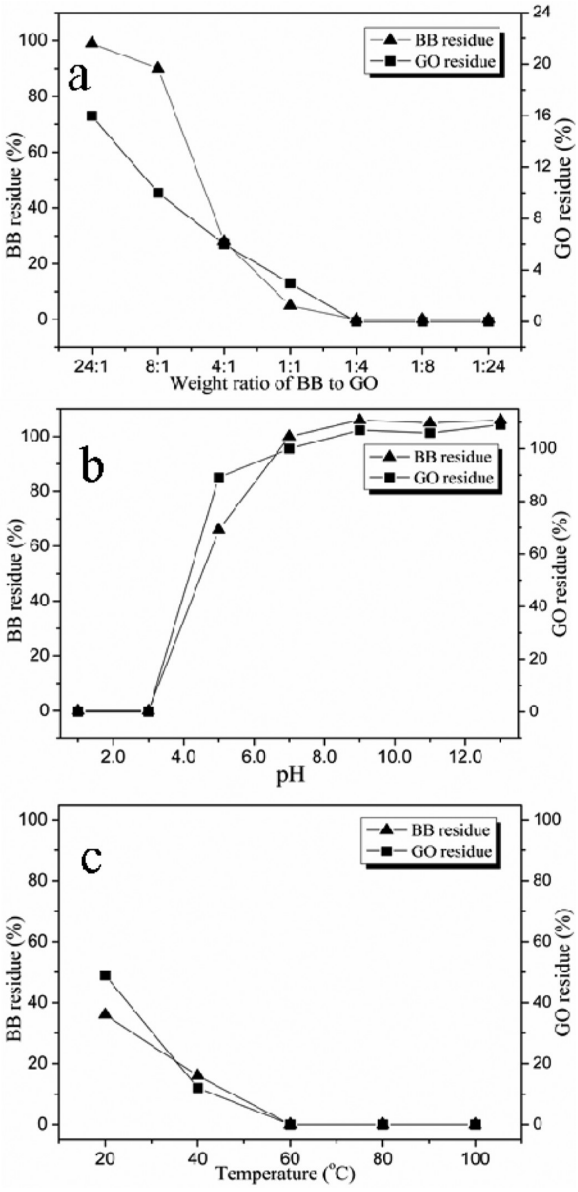

Figure 6. Influence factors on the coagulation of AC/BBGO after adsorption with the initial AC concentration of 10 mg/L and BBGO concentration of 25 mg/L. (a) W_{BB}:W_{GO} = 24:1, 8:1, 4:1, 1:1, 1:4, 1:8, and 1:24 (pH 3.0, 60 °C); (b) pH of 1.0, 3.0, 5.0, 7.0, 9.0, 11.0, 13.0 (W_{BB}:W_{GO} = 1:24, 60 °C); (c) temperature of 20, 40, 60, 80, 100 °C (W_{BB}:W_{GO} = 1:24, pH 3.0).

temperature from 20 to 100 °C, implying the increase of the coagulation performance, as high temperature facilitated the collisions of BB and GO colloidal particles. At temperature of 60, 80, and 100 °C, neither BB nor GO remained in the supernatant after coagulation. From the aspect of energy saving, 60 °C was the optimum temperature for the coagulation of BBGO. Overall, the parameters (W_{BB}:W_{GO} = 1:24, pH 3.0 and 60 °C) were proved to be optimal for the coagulation of BBGO.

3.3. Adsorption Performance Investigation. *3.3.1. Adsorption of AC.* The adsorption capacity of BBGO for AC was investigated compared with GO as well as BB. The results showed that the AC removal efficiency by both BBGO and GO increased with time (Figure 7). However, BB showed a relatively steady adsorption-time trend during the entire

dx.doi.org/10.1021/am4002666 | ACS Appl. Mater. Interfaces 2013, 5, 4783−4790

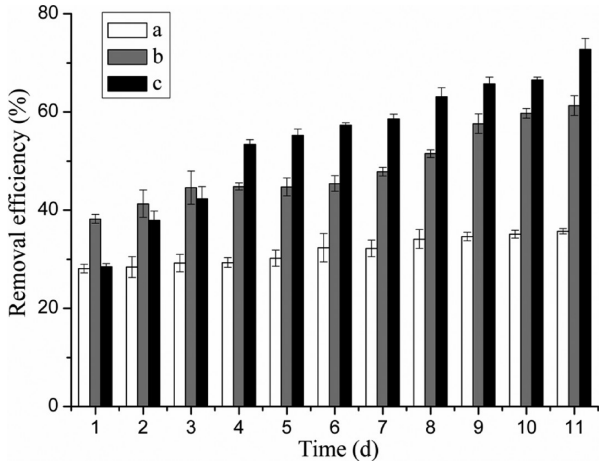

Figure 7. Removal efficiency of (a) BB (1 mg/L), (b) GO (24 mg/L), and (c) BBGO (25 mg/L, W_{BB}:W_{GO} = 1:24) for AC (initial concentration of 10 mg/L) after adsorption for 11 days.

process. Furthermore, the adsorption ability of BBGO was lower than that of GO during the initial 3 days. Nevertheless, from the fourth to 11th day, the adsorption performance of BBGO increased obviously and exceeded that of GO more and more significantly with time. This was probably due to the relatively higher specific surface area and stability of BBGO in aqueous solution. On the 11th day, the removal efficiency of AC by BBGO could reach approximately 72% with the adsorption capacity of 1.676 mmol/g. While the maximum removal efficiencies of BB and GO on AC were just 35.7 and 61.3%, which were obviously lower than that of BBGO. That was to say, BB played a role in the improvement of the adsorption capacity of GO.

3.3.2. Influence of Initial AC Concentration. Effect of initial AC concentration on AC removal by BBGO was studied by carrying out the experiments at different initial concentrations (1, 4, 7, 10 mg/L) keeping pH (7.0), stirring speed (150 rpm), temperature (25 °C) constant and varying the contact time (2, 4, 6, 8, 12, 24, 48, 84, 132, 192, and 264 h). The effect of initial concentration on AC removal efficiency was shown in Figure 8. When initial concentration of AC increased from 1 to 10 mg/L, the AC removal efficiency of 25 mg/L BBGO decreased from 92.5 to 70.5% at contact time of 264 h. Although the adsorption

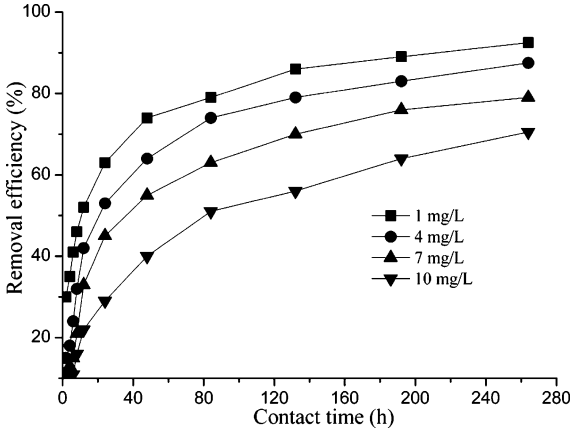

Figure 8. Effect of initial AC concentration on AC removal by 25 mg/L BBGO at pH 7.0.

capacity was found to be increased from 0.213 to 1.625 mmol/g.

3.3.3. Adsorption of FL. In comparison with GO and BB, the adsorption capacity of BBGO for FL was also investigated. The results showed that the removal efficiency of FL by BBGO could reach 93.2% with adsorption capacity of 2.212 mmol/g, while the removal efficiencies of FL by BB and GO were approximately 30 and 62% respectively. Therefore, the order of adsorption capacity was BBGO > GO > BB for FL (Figure 9),

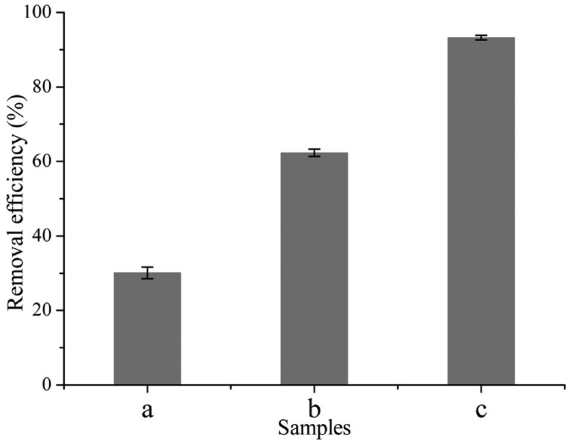

Figure 9. Removal efficiency of (a) BB (1 mg/L), (b) GO (24 mg/L), and (c) BBGO (25 mg/L, W_{BB}:W_{GO} = 1:24) for FL (initial concentration of 10 mg/L) after adsorption for 100 min.

and the same order could be deduced from Figure 7 for AC, illustrating that the adsorption mechanisms of both AC and FL were probably similar. Compared with AC, the adsorption process of FL seemed faster, which just took approximately two hours to reach removal efficiency above 93%. From the SEM images of AC/BBGO and FL/BBGO (Figure 1d, e), we could deduce that FL might have better attachment ability onto BB surface than AC, which was probably because the attachment force ($\pi-\pi$ stacking) between FL and BB was stronger than that between AC and BB resulting from the structural differences between FL and AC molecules.

3.3.4. Influence of Initial FL Concentration. Effect of initial FL concentration on FL removal by BBGO was also studied at the same conditions as adsorption of AC except the varying contact time (5, 10, 20, 30, 40, 50, 60, 80, and 100 min). The effect of initial concentration on FL removal efficiency was shown in Figure 10. When initial concentration of FL increased from 1 to 10 mg/L, the FL removal efficiency of 25 mg/L BBGO decreased from 99.0 to 92.5% at contact time of 100 min, whereas the adsorption capacity was found to increase from 0.235 to 2.196 mmol/g, which is similar to the adsorption of AC.

The adsorption capacity of BBGO to PAHs (1.676 mmol/g for anthracenemethanol and 2.212 mmol/g for fluoranthene) was compared with other adsorbents reported previously (0.128−2.4 mmol/g), seen in Table 1. Among these adsorbents, BBGO seemed to own moderate adsorption capacity, but AC/BBGO and FL/BBGO could be flocculated conveniently under appropriate conditions (pH 3.0 and temperature of 60 °C). This solid-liquid separation approach (namely coagulation) was utilized after adsorption and proved to be facile and unique compared with the reported. Moreover, little secondary pollution was introduced to the system in the

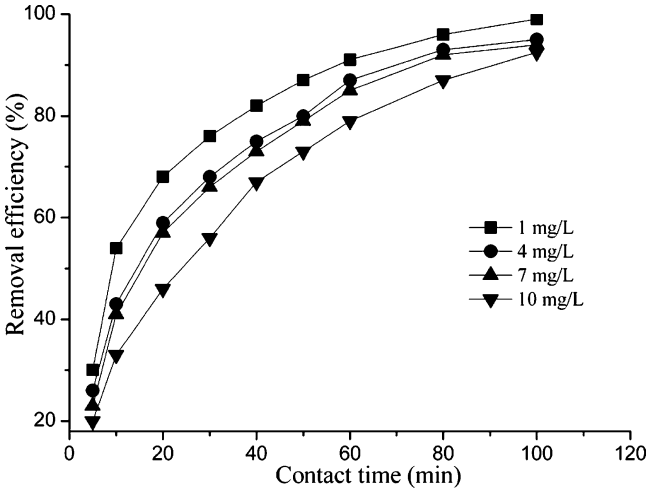

Figure 10. Effect of initial FL concentration on FL removal by 25 mg/L BBGO at pH 7.0.

Table 1. Comparison of the Maximum Removal Capacities of Different PAHs

adsorbents	adsorbates (PAHs)	adsorption capacity (mmol/g)	ref
mesoporous silica	naphthalene	0.136	30
natural bentonite	2-naphthol	0.128	31
multiwalled carbon nanotubes	1-naphthol	0.377	32
activated carbon	naphthalene	0.805	30
sulfonated graphene	naphthalene and 1-naphthol	2.3–2.4	15
functional graphene oxide	fluoranthene	2.212	this work
functional graphene oxide	anthracenemethanol	1.676	this work

removal process because it was not necessary to use any flocculant. Therefore, BBGO could be used as a promising adsorbent for PAHs, and this removal approach was environmentally friendly.

3.4. Adsorption Mechanism. The adsorption mechanism of AC or FL onto BBGO was deduced based on the preceding SEM, FTIR and Raman analysis. From images d and e in Figure 1, after adsorption of AC or FL, the surface of BBGO was attached by AC or FL molecules, which could be used to explain the batch adsorption experiments results. According to the FTIR and Raman analysis, AC or FL might be adsorbed onto BBGO by $\pi-\pi$ stacking interactions or hydrogen bonding. Therefore, the adsorption mechanism could be graphically represented as Figure 11.

4. CONCLUSION

In summary, GO was modified with BB through weak interaction forces ($\pi-\pi$ stacking or hydrogen bonding) and thus BBGO was obtained. It was found that BBGO possessed higher stability as well as removal efficiency for AC or FL in aqueous solution compared with GO. Moreover, a facile and unique solid-liquid separation approach was developed. After adsorption, AC/BBGO or FL/BBGO could be removed conveniently through coagulation which could be controlled by pH and temperature without introduction of any flocculant or further treatment (filtration or centrifugation). In a word,

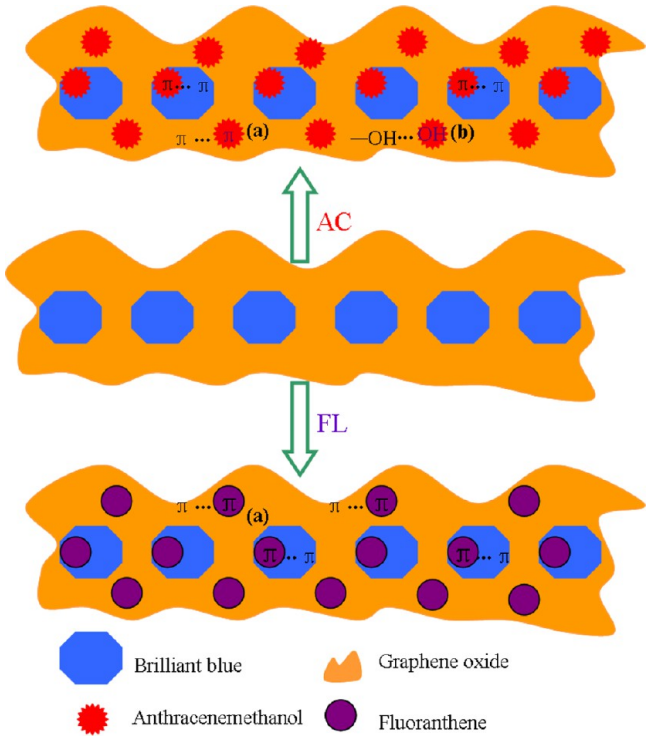

Figure 11. Adsorption schematic diagrams of FL or AC on BBGO though (a) $\pi-\pi$ EDA interactions, (b) hydrogen bonding.

this work provided a promising adsorbent for PAHs as well as a facile and environmentally friendly removal approach.

■ ASSOCIATED CONTENT

Supporting Information

BET specific surface area and stability experimental results. This material is available free of charge via the Internet at http://pubs.acs.org.

■ AUTHOR INFORMATION

Corresponding Author

*Corresponding author. Tel.: +86-551-65595012; Fax: +86-551-65591413. E-mail: zywu@ipp.ac.cn.

Notes

The authors declare no competing financial interest.

†C.Z. and L.W. are co-first authors.

■ ACKNOWLEDGMENTS

The authors acknowledge financial support from the National Natural Science Foundation of China (10975154) and Scientific and Technological Project of Anhui Province (1206c0805014).

■ REFERENCES

(1) Santoro, A.; Modica, R.; Paglialunga, S.; Bartošek, I. *Toxicol. Lett.* **1979**, *3*, 85–93.
(2) Haritash, A. K.; Kaushik, C. P. *J. Hazard. Mater.* **2009**, *169*, 1–15.
(3) Gu, M. B.; Chang, S. T. *Biosens. Bioelectron.* **2001**, *16*, 667–674.
(4) Bernal-Martínez, A.; Carrère, H.; Patureau, D.; Delgenès, J. P. *Process Biochem.* **2005**, *40*, 3244–3250.
(5) Gan, S.; Lau, E. V.; Ng, H. K. *J. Hazard. Mater.* **2009**, *172*, 532–549.
(6) Zheng, X. J.; Blais, J. F.; Mercier, G.; Bergeron, M.; Drogui, P. *Chemosphere* **2007**, *68*, 1143–1152.

(7) Bernal-Martinez, A.; Carrère, H.; Patureau, D.; Delgenès, J. P. *Chemosphere* **2007**, *68*, 1013−1019.
(8) Vidal, C. B.; Barros, A. L.; Moura, C. P.; de Lima, A. C. A.; Dias, F. S.; Vasconcellos, L. C. G.; Fechine, P. B. A.; Nascimento, R. F. *J. Colloid Interface Sci.* **2011**, *357*, 466−473.
(9) Nkansah, M. A.; Christy, A. A.; Barth, T.; Francis, G. W. *J. Hazard. Mater.* **2012**, *217−218*, 360−365.
(10) Yuan, M.; Tong, S.; Zhao, S.; Jia, C. Q. *J. Hazard. Mater.* **2012**, *181*, 1115−1120.
(11) Ma, J.; Zhu, L. *J. Hazard. Mater.* **2006**, *B136*, 982−988.
(12) Gong, Z.; Alef, K.; Wilke, B. M.; Li, P. *J. Hazard. Mater.* **2007**, *143*, 372−378.
(13) Bruna, F.; Celis, R.; Real, M.; Cornejo, J. *J. Hazard. Mater.* **2012**, *225−226*, 74−80.
(14) Yang, K.; Zhu, L.; Xing, B. *Environ. Sci. Technol.* **2006**, *40*, 1855−1861.
(15) Zhao, G. X.; Jiang, L.; He, Y. D.; Li, J. X.; Dong, H. L.; Wang, X. K.; Hu, W. P. *Adv. Mater.* **2011**, *23*, 3959−3963.
(16) Liu, H.; Deng, H.; Liu, Z. *Tech. Water Treat.* **2010**, *36*, 1−5.
(17) Dai, Y.; Yin, L.; Niu, J. *Environ. Sci. Technol.* **2011**, *45*, 10611−10618.
(18) Manoli, E.; Samara, C. *Environ. Pollut.* **2008**, *151*, 477−485.
(19) López-Vizcaíno, R.; Sáez, C.; Cañizares, P.; Rodrigo, M. A. *Sep. Purif. Technol.* **2012**, *88*, 46−51.
(20) Cai, X.; Tan, S.; Lin, M.; Xie, A.; Mai, W.; Zhang, X.; Lin, Z.; Wu, T.; Liu, Y. *Langmuir* **2011**, *27*, 7828−7835.
(21) Song, H. S.; Ko, C. H.; Ahn, W. *Ind. Eng. Chem. Res.* **2012**, *51*, 10259−10264.
(22) Xu, J.; Wang, L.; Zhu, Y. *Langmuir* **2012**, *28*, 8418−8425.
(23) Hummers, W. S.; Offeman, R. E. *J. Am. Chem. Soc.* **1958**, *80*, 1339−1339.
(24) Lu, C. H.; Yang, H. H.; Zhu, C. L.; Chen, X.; Chen, G. N. *Angew. Chem., Int. Ed.* **2009**, *48*, 4785−4787.
(25) Lu, C.; Li, J.; Zhang, X. *Anal. Chem.* **2011**, *83*, 7276−7282.
(26) Li, Y. H.; Du, Q. J.; Liu, T. H.; Peng, X. J.; Wang, J. J.; Sun, J. K.; Wang, Y. H.; Wu, S. L.; Wang, Z. H.; Xia, Y. Z.; Xia, L. H. *Chem. Eng. Res. Des.* **2013**, *91*, 361−368.
(27) Ji, Q. M.; Guo, C. Y.; Yu, X. Y.; Ochs, C. J.; Hill, J. P.; Caruso, F.; Nakazawa, H.; Ariga, K. *Small* **2012**, *8*, 2345−2349.
(28) Xu, Z. H.; Qiu, F. S.; Jiang, Y.; Niu, H. B.; Chen, X. W.; Huang, X. G. *J. Xi'an Jiaotong Univ.* **2007**, *41*, 746−749.
(29) Yang, Z.; Yuan, B.; Huang, X.; Zhou, J.; Cai, J.; Yang, H.; Li, A.; Cheng, R. *Water Res.* **2012**, *46*, 107−114.
(30) Anbia, M.; Moradi, S. E. *Korean J. Chem. Eng.* **2012**, *29*, 743−749.
(31) Wei, J. M.; Zhu, R. L.; Zhu, J. X.; Ge, F.; Yuan, P.; He, H. P.; Ming, C. *J. Hazard. Mater.* **2009**, *166*, 195−199.
(32) Sheng, G. D.; Shao, D. D.; Ren, X. M.; Wang, X. Q.; Li, J. X.; Chen, Y. X.; Wang, X. K. *J. Hazard. Mater.* **2010**, *178*, 505−516.